

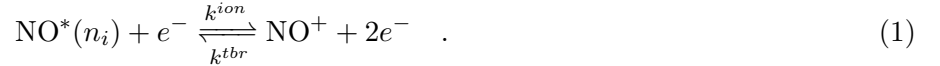
# Coupled rate-equation model for the avalanche, bifurcation and quench of the nitric oxide molecular ultracold plasma

January 25, 2022

## 1 State-detailed kinetic mechanism for avalanche to plasma and quench

### 1.1 Mechanism

The plasma forms as the result of an avalanche of ionizing Rydberg-electron collisions described by a second-order rate constant  $k_i^{ion}$ . Three-body-recombination, with rate constant  $k_i^{tbr}$ , reverses this process:



Both rate constants depend on electron temperature and vary with  $n_i$ , the principal quantum number of  $\text{NO}^*$ .

Rydberg-electron collisions,  $k_{ij}$ , scramble the initial state of  $\text{NO}^*$ , exchanging binding energy with electron thermal motion:



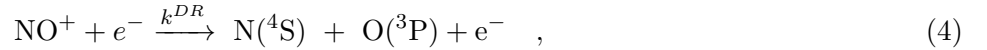
In a molecular Rydberg gas, dissociation affects plasma evolution.

Predissociation of  $\text{NO}^*$ ,



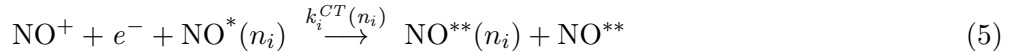
diminishes plasma density and consumes binding energy.

Direct dissociative recombination,



reduces the balanced population of electrons and ions.

Hydrodynamic charge exchange with electron-ion recombination (CT bifurcation accompanied by electron quench) consumes inner-shell ions as they expand through stationary outer shells of Rydberg gas.



Note that the magnitude of  $k_{CT}(n_i)$  depends on  $n_i$ . And, charge exchange conserves Rydberg principal quantum number. But, we regard those Rydberg formed by this process as special. They do not predissociate, nor do they undergo electron impact ionization. In effect, charge exchange exhausts the thermal energy of the associated free electron, quenching it to form a companion pair of high- $\ell$  molecules, one that conserves the reactant principal quantum number,  $\text{NO}^{**}(n_i)$ , and a companion in some very high- $n$ , high- $\ell$  state.

## 1.2 Master equations describing avalanche and charge transfer in a plasma of uniform plasma density

We define  $\rho_i = \text{NO}^*(n_i)$  as the density of Rydberg molecules with principal quantum number  $n_i$  in a plasma of uniform density. Let  $\rho_e = n_e$  represent the density of free electrons. We also use  $\rho_e$  to designate the density of  $[\text{NO}^+]$  ions, which remain always in balance by quasi-neutrality, which is to say,  $\rho_e = n_e = [\text{NO}^+]$ . As indicated in Eq (5) hydrodynamic charge exchange forms a subset of quenched Rydberg molecules at each principal quantum number,  $n_i$  with an evolving density defined by  $\rho_i^{**}$ .

Note, here because both the quenched  $\text{NO}^{**}(n_i)$  molecules and  $\text{NO}^+$  ions close-coupled electron pairs form in a regime of suppressed electron collisions, we assume that no inelastic electron -  $\text{NO}^{**}$  collisions of consequence occur, leading either to Rydberg states of different  $n_i$  or free, unassociated  $\text{NO}^+$  ions and electrons. Thus, we drop the principal quantum number label for coupled rate calculations and simply say that  $\rho^{**} = [\text{NO}^{**}] = 2 \sum_i \rho_i^{**}$ . Note, in this picture,  $[\text{NO}^{**}]$  forms a sink filled by conversion from ions and Rydberg molecules from which no outlet exists in the absence of an additional source of dissipation.

For a uniform density,  $\rho_i$ , of Rydberg molecules in state  $n_i$  and electron density,  $\rho_e$  the rate processes represented by Eqs. 1 to 5 yield the system of coupled rate equations:

$$\begin{aligned} \frac{d\rho_i}{dt} &= -\rho_i\rho_e \sum_j k_{ij} + \rho_e \sum_j k_{ji}\rho_j - k_i^{\text{ion}}\rho_i\rho_e + k_i^{\text{tbr}}\rho_e^3 - k_i^{\text{PD}}\rho_i - k_i^{\text{CT}}\rho_i\rho_e \\ \frac{d\rho_e}{dt} &= \rho_e \sum_i k_i^{\text{ion}}\rho_i - \rho_e^3 \sum_i k_i^{\text{tbr}} - k^{\text{DR}}\rho_e^2 - \rho_e \sum_i k_i^{\text{CT}}\rho_i \\ \frac{d\rho^{**}}{dt} &= \rho_e \sum_i k_i^{\text{CT}}\rho_i \end{aligned} \quad (6)$$

where we use quasi-neutrality to set  $\rho_{\text{ion}}$  equal to  $\rho_e$ . Introducing the density of dissociated molecules  $\rho^{\text{DR}}$ ,  $\rho_i^{\text{PD}}$  owing to recombination and predissociation together with the total density of quenched  $\text{NO}^{**}$  Rydberg molecules, defined by a quantity  $\rho^{**} = 2 \sum_i \rho_i^{**}$ , defines a conserved number of NO-associated particles,  $N$  ( $\text{NO}^+$  ion - electron pairs,  $\text{NO}^*$  and  $\text{NO}^{**}$  Rydberg molecules and sets of  $\text{N}(^4\text{S}) + \text{O}(^3\text{P})$  atomic dissociation products):

$$N/V = \rho_e + \rho^{\text{DR}} + \sum_i (\rho_i + \rho_i^{\text{PD}}) + \rho^{**} \quad (7)$$

In principal, the dynamics extend over an infinite range of quantum numbers  $n_i$ . In practice, however, we define a lower bound of  $n_{\min} = 10$  and set the upper bound to  $n_{\max} = \sqrt{R/k_B T}$ , which conforms best with plasma scaling. [1].

## 1.3 Time evolution of electron temperature in a plasma of uniform density

Considering the global conservation of total energy coupled with the rapid collisional equilibration of electron kinetic energy, the electron temperature in a plasma of uniform density evolves as:

$$0 = \frac{d}{dt} E_{\text{tot}} = \frac{d}{dt} \left( \frac{3}{2} k_B T_e(t) \rho_e - R \sum_i \frac{\rho_i}{n_i^2} - E_{\text{loss}} \right) \quad , \quad (8)$$

where  $E_{\text{loss}}$  describes the energy loss per unit volume owing to the dissociation of NO to form  $\text{N}(^4\text{S}) + \text{O}(^3\text{P})$ , and charge transfer sequestering NO molecules in the bifurcated volumes of quenched high-Rydberg  $\text{NO}^{**}$

molecules:

$$E_{loss} = -\frac{3}{2}k_B \int_{t_0}^t dt' T_e(t') \dot{\rho}_e^{DR}(t') + R \sum_i \frac{\rho_i^{PD}}{n_i^2} + R \sum_i \frac{\rho_i^{**}}{n_i^2}. \quad (9)$$

This expression for energy conservation assumes that no change in the potential energy of the system accompanies the formation of close-coupled  $\text{NO}^+$  ion - electron pairs via reaction (5).

#### 1.4 Plasma evolution in a Gaussian ellipsoidal density distribution represented by 100 concentric shells

We account explicitly for the prolate distribution of plasma density by defining a Gaussian ellipsoid with semi-axes  $r_k = 5\sigma_k$  ( $k = x, y, z$ ), divided into  $L = 100$  concentric ellipsoidal shells with walls separated by equal widths along the principal axes.

At  $t = 0$ , each shell accounts for a defined uniform initial density of Rydberg NO molecules. Taken together, these shells describe the discretized initial distribution of the Rydberg gas. A separate set of coupled rate equations (Eq. 6) describes the evolution of Rydberg gas to plasma in each shell, as labeled by the superscript index  $\alpha = 1, \dots, L$ :

$$\begin{aligned} \frac{d\rho_i^\alpha}{dt} &= -\rho_i^\alpha \rho_e^\alpha \sum_j k_{ij} + \rho_e^\alpha \sum_j k_{ji} \rho_j^\alpha - k_i^{ion} \rho_i^\alpha \rho_e^\alpha + k_i^{tbr} (\rho_e^\alpha)^3 - k_i^{PD} \rho_i^\alpha - k_i^{CT} \rho_i^{\alpha+1} \rho_e^\alpha \\ \frac{d\rho_e^\alpha}{dt} &= \rho_e^\alpha \sum_i k_i^{ion} \rho_i^\alpha - (\rho_e^\alpha)^3 \sum_i k_i^{tbr} - k^{DR} (\rho_e^\alpha)^2 - \rho_e^\alpha \sum_i k_i^{CT} \rho_i^{\alpha+1} \\ \frac{d\rho^{\alpha**}}{dt} &= \rho_e^\alpha \sum_i k_i^{CT} \rho_i^{\alpha+1} \end{aligned} \quad (10)$$

At the density of the molecular beam, the recoiling neutral  $\text{N}(^4\text{S}) + \text{O}(^3\text{P})$  products of nitric oxide dissociation have a mean free path that is much larger than the entire plasma volume [2]. The electrons on the other hand are bound by the space charge of the ions. The volume occupied by the ions produced in a given shell define the evolving volume of that shell. Thus, we assume that the constraint of quasi-neutrality confines the corresponding electrons to the same volume. The low electron mass ensures a fast kinetic energy transfer between electrons in all shells, which we assume instantaneously equilibrates the electron temperature,  $T_e^\alpha = T_e^{\alpha'} = T_e$ . As a consequence, energy conservation holds for the ellipsoid as a whole:

$$0 = \frac{d}{dt} \sum_\alpha E_{tot}^\alpha(t) V^\alpha = \frac{d}{dt} \left( \frac{3}{2} k_B T_e(t) \sum_\alpha \rho_e^\alpha V^\alpha - R \sum_{i\alpha} \frac{\rho_i^\alpha}{n_i^2} V^\alpha - \sum_\alpha E_{loss}^\alpha V^\alpha \right). \quad (11)$$

Equations 10-11 form a set of  $(n_{max} - n_{min} + 2)L + 1$  ordinary differential equations which we solve by numerical integration.

#### 1.5 Hydrodynamic Shell Model

The Vlasov equations provide an effective means of describing the expansion of a spherical Gaussian plasma [3,4]. In earlier work, we have applied the analytical Vlasov equation approach to describe the collisionless expansion of a Gaussian ellipsoidal plasma, and confirmed that the results match with an ellipsoidal shell-model numerical solution [2,5]. Here, we extend this approach to capture the effect of electron energy loss owing to expansion on the collisional dynamics of plasma avalanche bifurcation and quench, in other words.

Under the conditions of simultaneous avalanche and expansion, the force of the expanding electron gas acts on the  $\text{NO}^+$  ions to increase the radial coordinates of the plasma, diminishing its density and reduce the electron temperature according to:

$$-m_i \frac{du}{dt} = e \nabla \Phi = k_B T_e \frac{\nabla \rho_e}{\rho_e} \quad , \quad (12)$$

where  $m_i$  represents the ion mass, and  $u$  the radial velocity. These effects of electron temperature and charged particle density have straightforward effects on the coupled rate processes ongoing in the shells.

We begin by neglecting any dynamical consequences of ion-ion and ion-Rydberg collisions, and model the hydrodynamic evolution of the plasma by the self-similar expansion of the Gaussian volume along its ellipsoidal axes,  $k$ , governed by the corresponding charge density gradients. The shell model of this ellipsoid defines these gradients discretely and enforces self-similarity by approximating,

$$-m_i \frac{d^2 r_k^\alpha}{dt^2} \approx k_B T_e \left\langle \frac{\nabla_k \rho_e}{\rho_e r_k} \right\rangle r_k^\alpha = k_B T_e \frac{1}{L} \sum_\beta \frac{1}{\rho_e^\beta r_k^\beta} \frac{\rho_e^{\beta+1} - \rho_e^\beta}{r_k^{\beta+1} - r_k^\beta} r_k^\alpha \quad . \quad (13)$$

Here,  $r_k^\alpha$  is the position of shell  $\alpha$  along the  $k$ -axis and brackets denote the average over all shells  $\alpha$ . The second equality figures the gradients in  $x$ ,  $y$ , and  $z$  discretely by summing the differences in adjacent charge densities over all cells.

Ambipolar expansion transfers electron kinetic energy to the radial motion of the ions. For simplicity, we assume three uncoupled energy channels as would be the case for a spherical distribution:

$$E_{kin}^\alpha \approx \frac{m_i}{2} \frac{(u_x^\alpha)^2 + (u_y^\alpha)^2 + (u_z^\alpha)^2}{3} \quad . \quad (14)$$

Adding this to the energy conservation Eq. 11 gives:

$$0 = \frac{d}{dt} \left( \frac{3}{2} k_B T_e(t) \sum_\alpha \rho_e^\alpha V^\alpha - R \sum_{i\alpha} \frac{\rho_i^\alpha}{n_i^2} V^\alpha - \sum_\alpha E_{loss}^\alpha V^\alpha + \sum_\alpha E_{kin}^\alpha V^\alpha \right) \quad . \quad (15)$$

Finally, we account for the rarefaction of the charge and Rydberg molecule distributions owing to expansion. Modifying Eq. 10 yields

$$\begin{aligned} \frac{d\rho_i^\alpha}{dt} &= -\rho_i^\alpha \rho_e^\alpha \sum_j k_{ij} + \rho_e^\alpha \sum_j k_{ji} \rho_j^\alpha - k_i^{ion} \rho_i^\alpha \rho_e^\alpha + k_i^{tbr} (\rho_e^\alpha)^3 - k_i^{PD} \rho_i^\alpha - k_i^{CT} \rho_i^{\alpha+1} \rho_e^\alpha - \frac{\rho_i^\alpha}{V^\alpha} \frac{dV^\alpha}{dt} \\ \frac{d\rho_e^\alpha}{dt} &= \rho_e^\alpha \sum_i k_i^{ion} \rho_i^\alpha - (\rho_e^\alpha)^3 \sum_i k_i^{tbr} - k^{DR} (\rho_e^\alpha)^2 - \rho_e^\alpha \sum_i k_i^{CT} \rho_i^{\alpha+1} - \frac{\rho_e^\alpha}{V^\alpha} \frac{dV^\alpha}{dt} \\ \frac{d\rho^{\alpha**}}{dt} &= \rho_e^\alpha \sum_i k_i^{CT} \rho_i^{\alpha+1} - \frac{\rho^{\alpha**}}{V^\alpha} \frac{dV^\alpha}{dt} \quad , \end{aligned} \quad (16)$$

where the volume of shell  $\alpha$  changes as

$$\frac{dV^\alpha}{dt} = \frac{4\pi}{3} \frac{d}{dt} \left( \prod_k r_k^\alpha - \prod_k r_k^{\alpha-1} \right) \quad . \quad (17)$$

We may now proceed to integrate Eq. 13-17.

## 1.6 Rate constants

We adopt expressions for rate constants,  $k_i^{ion}$ ,  $k_i^{tvr}$ ,  $k_{ij}$  as functions of electron temperature developed with reference to Monte Carlo trajectory simulations by Pohl and coworkers [6]. Generally speaking, all of these rate constants increase as orbital radius grows with  $n$ . High electron temperature favours ionization and suppresses recombination. Values of  $k_{ij}$  peak for transitions to neighbouring states. At high electron temperatures,  $n$ -changing collisions drive upward transitions more frequently than transitions down. Lower temperatures reverse this effect. This relationship between the electron temperature and the net flux of Rydberg binding energy supports the formation of a quasi-equilibrium distribution of high-Rydberg molecules, ions and electrons at a temperature that depends on the density of the system. Hydrodynamic expansion reduces electron temperature and thereby links the position of the quasi-equilibrium to evolution in the radial coordinates of the system.

We calculate a rate constant for dissociative recombination  $k^{DR}$  based on the model of Schneider *et al.* [7].  $k^{DR}(T_e)$  fits a power-law in temperature with exponent  $-0.51$ . Values of  $k^{PD}$  vary with  $n$  and  $l$  according to our previously introduced model [1]. In this picture, the increasing volume of Rydberg orbitals with principal quantum number decreases the predissociation rate by a factor of  $n^{-3}$ . The predissociation rate also depends on orbital momentum,  $l$ . For present purposes, we assume intrinsic rates  $k_l = 0.014, 0.046, 0.029, 0.0012$  for  $l = 0$  to  $3$  and  $k_{l \geq 4} = 3 \times 10^{-5}$  as compiled by Gallagher *et al* [8] and Bixon and Jortner [9]. Electron collisions drive transitions between orbital momentum states, randomizing the  $l$ - and  $m_l$ -distribution [10]. Statistical dilution further decreases  $k_i^{PD}$  by a factor of  $n_i^{-2}$  to yield:

$$k_i^{PD} = \frac{\sum_{l=0}^{n_i-1} (2l+1) k_l}{n_i^2} \frac{4.13 \times 10^7 \text{ ns}^{-1}}{2\pi n_i^3} \quad (18)$$

For  $n = 49$ , Eq. 18 yields a lifetime  $\tau = (k_{i=49}^{PD})^{-1} = 114 \text{ ns}$ . Radiative decay is usually slower than predissociation and can thus be neglected [10]. Experimental lifetimes of  $nf(2)$ -Rydberg states measured by Vrakking and Lee agree reasonably with this model [11].

Rate of  $\text{NO}^+ - \text{NO}^*$  charge exchange depends proportionally on the square of the principal quantum number of the target Rydberg molecule.

## 1.7 Indirect hydrodynamic expansion of the neutralized products of charge-exchange

Figure shells into which put  $\text{NO}^{**}$  molecules.

Start with empty shells superimposed on Rydberg gas shells.

As ion shells expand, CT produces  $\text{NO}^{**}$ . Add to appropriate shells. Expand with one-half the velocity of corresponding ion shell. With every two steps of hydrodynamic ion advance, advance the  $\text{NO}^{**}$  shells by one step.

## References

- [1] Saquet N, Morrison JP, Grant E: **Recombinative dissociation and the evolution of a molecular ultracold plasma.** *Journal of Physics B: Atomic, Molecular and Optical Physics* 2012, **45**(17):175302.
- [2] Schulz-Weiling M, Sadeghi H, Hung J, Grant E: **On the evolution of the phase-space distributions of a non-spherical molecular ultracold plasma in a supersonic beam.** *Journal of Physics B: Atomic, Molecular and Optical Physics* 2016, **49**(19):193001.
- [3] Dorozhkina DS, Semenov VE: **Exact Solution of Vlasov Equations for Quasineutral Expansion of Plasma Bunch into Vacuum.** *Physical review letters* 1998, **81**(13):2691–2694.

- [4] Killian TC, Pattard T, Pohl T, Rost JM: **Ultracold neutral plasmas**. *Physics Reports* 2007, **449**(4-5):77–130.
- [5] Sadeghi H, Grant ER: **Dissociative recombination slows the expansion of a molecular ultracold plasma**. *Physical Review A* 2012, **86**(5):052701.
- [6] Pohl T, Vrinceanu D, Sadeghpour HR: **Rydberg atom formation in ultracold plasmas: small energy transfer with large consequences**. *Physical review letters* 2008, **100**(22):223201.
- [7] Schneider IF, Rabadán I, Carata L, Andersen LH, Suzor-Weiner A, Tennyson J: **Dissociative recombination of  $\text{NO}^+$ : Calculations and comparison with experiment**. *Journal of Physics B: Atomic, Molecular and Optical Physics* 2000, **33**(21):4849, [<http://iopscience.iop.org/article/10.1088/0953-4075/33/21/326/pdf>].
- [8] Murgu E, Martin JDD, Gallagher TF: **Stabilization of predissociating nitric oxide Rydberg molecules using microwave and radio-frequency fields**. *The Journal of Chemical Physics* 2001, **115**(15):7032–7040.
- [9] Bixon M, Jortner J: **The dynamics of predissociating high Rydberg states of NO**. *The Journal of Chemical Physics* 1996, **105**(4):1363–1382.
- [10] Chupka WA: **Factors affecting lifetimes and resolution of Rydberg states observed in zero-electron-kinetic-energy spectroscopy**. *The Journal of Chemical Physics* 1993, **98**(6):4520–4530.
- [11] Vrakking MJJ, Lee YT: **Lifetimes of Rydberg states in zero-electron-kinetic-energy experiments. I. Electric field induced and collisional enhancement of NO predissociation lifetimes**. *The Journal of Chemical Physics* 1995, **102**(22):8818–8832.